Biochemical and Biophysical Research Communications 458 (2015) 429–434

Contents lists available at ScienceDirect

Biochemical and Biophysical Research Communications

journal homepage: www.elsevier.com/locate/ybbrc

Crystal structure and function of an unusual dimeric Hsp20.1 provide insight into the thermal protection mechanism of small heat shock proteins

Liang Liu [a], Jiyun Chen [b], Bo Yang [a], Yonghua Wang [c, *]

[a] School of Bioscience and Bioengineering, South China University of Technology, Guangzhou 510006, China
[b] Institute of Systems Biomedicine and Department of Biophysics, School of Basic Medical Sciences, Peking University Health Science Center, Beijing 100191, China
[c] College of Light Industry and Food Sciences, South China University of Technology, Guangzhou 510641, China

ARTICLE INFO

Article history:
Received 14 January 2015
Available online 7 February 2015

Keywords:
Small heat shock protein (sHSP)
Crystal structure
Dimerization
Chaperone activity

ABSTRACT

Small heat shock proteins (sHSPs) are ubiquitous chaperones that play a vital role in protein homeostasis. sHSPs are characterized by oligomeric architectures and dynamic exchange of subunits. The flexible oligomeric assembling associating with function remains poorly understood. Based on the structural data, it is certainly agreed that two dimerization models depend on the presence or absence of a β6 strand to differentiate nonmetazoan sHSPs from metazoan sHSPs. Here, we report the *Sulfolobus solfataricus* Hsp20.1 ACD dimer structure, which shows a distinct dimeric interface. We observed that, in the absence of β6, Hsp20.1 dimer does not depend on β7 strand for forming dimer interface as metazoan sHSPs, nor dissociates to monomers. This is in contrast to other published sHSPs. Our structure reveals a variable, highly polar dimer interface that has advantages for rapid subunits exchange and substrate binding. Remarkably, we find that the C-terminal truncation variant has chaperone activity comparable to that of wild-type despite lack of the oligomer structure. Our further study indicates that the N-terminal region is essential for the oligomer and dimer binding to the target protein. Together, the structure and function of Hsp20.1 give more insight into the thermal protection mechanism of sHSPs.

1. Introduction

Protein damage resulting from stress causes breakdown of protein homeostasis [1]. There are multiple response mechanisms that protect cells against environment stress [2,3]. A 'protein quality control' network consisting of molecular chaperones and proteases is responsible for limiting and repairing protein aggregation [1]. The small heat shock proteins (sHSPs) are considered its important components. sHSPs are ubiquitous, diverse molecular chaperones that contribute to maintain protein homeostasis by preventing protein aggregation during heat shock [4]. The sHSPs' chaperone function is crucial to the cell's tolerance to stress, and their malfunction is implicated in a range of human pathologies [5,6]. Defects in sHSPs are linked to multiple inherited human diseases that are associated with protein misfolding, such as cataract, neuropathies, Alzheimer's disease, Parkinson's disease and multiple sclerosis [4].

sHSPs share a common architecture, which is characterized by the presence of a signature α-crystallin domain (ACD). This central domain is flanked by highly variable N- and C-terminal extensions [7]. A bioinformatics analysis of multiple sHSP sequences has revealed that the ACD with an average length of 94 residues typically composes the bulk of the sequence [5]. Despite low sequence identity, the ACD is the most conserved region of the sHSP sequence. The C-terminus with an average length of 10 residues contains a conserved IXI motif, which is defined as two Ile (or Val) residues separated by one residue. Nuclear magnetic resonance (NMR) and crystal structural studies reveal that the IXI motif on the C-terminal tail can interact with a hydrophobic region on an adjacent ACD [8]. The interaction takes place among neighboring dimers, facilitating the oligomer structure formation. Mutations or deletions of the C-terminal IXI motif residues result in a loss of

* Corresponding author. College of Light Industry and Food Sciences, South China University of Technology, 381 Wushan Road, Tianhe District, Guangzhou 510641, China. Fax: +86 020 87113842.
E-mail address: yonghw@scut.edu.cn (Y. Wang).

http://dx.doi.org/10.1016/j.bbrc.2015.01.134
0006-291X/

higher order oligomeric structure in multiple sHSPs by abrogating the ACD-IXI/V interaction [9]. The N-terminal region displays sequence variation and almost no sequence conservation between different sHSPs [10]. The structural data indicate that the N-terminal arm is an intrinsically flexible or disordered domain that may contribute to recognize and bind a wide range of target proteins [11,12]. Mutations or deletions of the N-terminal arm appear to affect the chaperone activities of sHSPs, implicating the N-terminal arm in substrate protection [13,14].

The molecular mass of the sHSP monomer is between 12 and 43 kDa [15]. The subunits of oligomers range from approximately 12 to >48. Although sHSPs show diversity of oligomer architecture, the dimer of ACD is the building block in all sHSP oligomers [16]. However, The ACD dimers of metazoan sHSPs show different dimerization model with that of nonmetazoans. In most determined plant, archaeal, and bacterial sHSPs structures, dimerization depend on the presence of a long loop that contains a β6 strand. The β6 strand exchanges between partner chains at the dimer interface [5,17]. In contrast, a very short loop is apparent in the mammalian sHSPs. The β6 strand has fused with β7 into an elongated "β6+7" strand, which forms the dimer interface in antiparallel orientation with the "β6+7" strand of the other monomer [18,19].

We have solved the X-ray structure of the ACD dimer of *Sulfolobus solfataricus* Hsp20.1, which exhibits model of dimerization different from that of metazoans and nonmetazoans. Although in the absence of β6, Hsp20.1 does not depend on β7 for forming dimer interface. We have observed variable dimer interfaces in sHSPs. In this study, we also determine that both the oligomer (wild-type) and the dimer (the C-terminal truncation variant) of Hsp20.1 can inhibit the thermal aggregation of malate dehydrogenase (MDH). Further functional investigation indicates that the long and disorder N-terminus is important for the chaperone activity of Hsp20.1 oligomer and dimer. Our structural and functional study of Hsp20.1 provides significant information for understanding the sHSP thermal protection mechanism.

2. Materials and methods

2.1. Expression, purification, crystallization, and data collection

Hsp20.1 wild-type and Hsp14.1 wild-type were expressed in *Escherichia coli* BL21 (DE3). Both proteins were soluble and existed in the supernatant of cell lysate. The supernatant was first heated at 75 °C for 30 min to remove thermally unstable host proteins. Then, the sHsps were successively purified by ion-exchange chromatography on a Resource Q 1/6 column (GE Healthcare Life Sciences) followed by size-exclusion chromatography on a Superdex 200 10/300 GL column (GE Healthcare Life Sciences). Variants were expressed and purified in the same way as the wild-type proteins.

Crystals of Hsp20.1 ACD (77-164) were grown at 20 °C by using the hanging-drop vapor diffusion method. Crystallization drop was a 1:1 mixture containing protein solution (16 mg/ml protein in

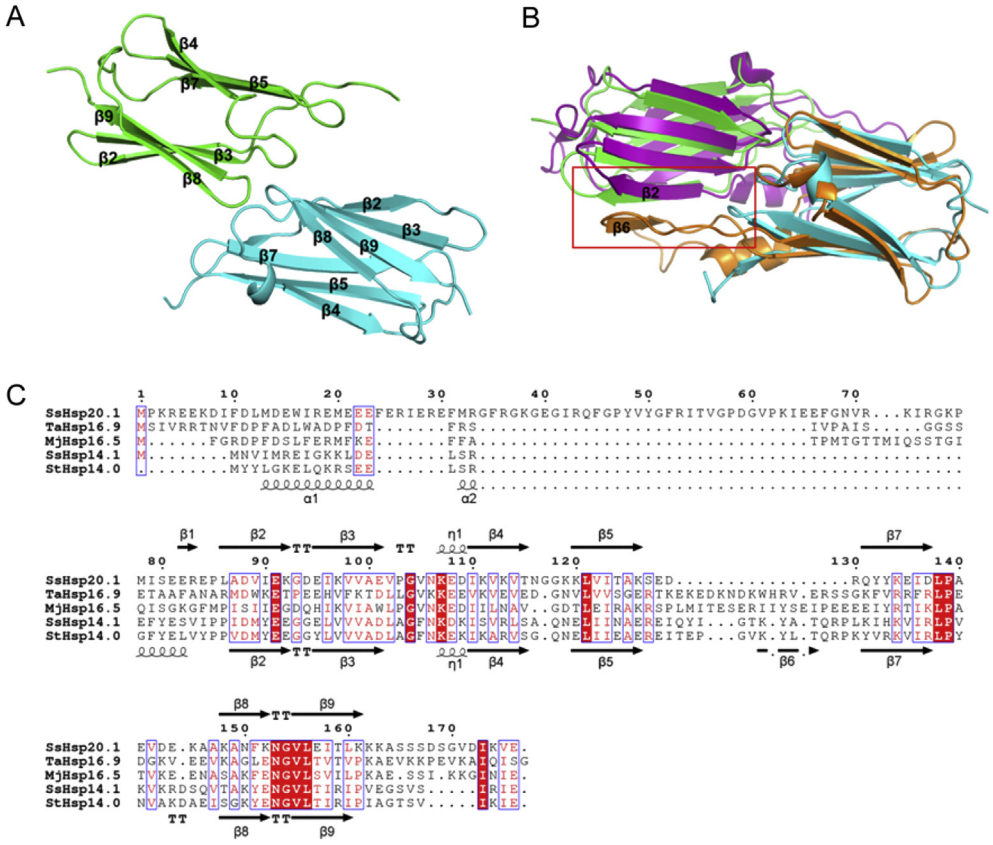

Fig. 1. Crystal structure of Hsp20.1. (A) The ACD dimer structure of Hsp20.1 is shown as a ribbon model. The A and B chain s are colored green and cyan, respectively. The notation of secondary structures is labeled in accord with *Methanocaldococcus jannaschii* Hsp16.5. (B) Superposition of the dimers of Hsp20.1 and *Sulfolobus tokodaii* Hsp14.0 (Protein Data Bank code 3AAB). The A and B chains in the Hsp20.1 dimer are colored green and cyan, while the A and B chains in the Hsp14.0 dimer are colored purple and orange. In the Hsp14.0 structure, β2 strand of A chain and β6 strand of B chain are noted. (C) Sequence alignment of sHsps. Alignment was generated using Promals3D and ESPript.3.0. Secondary structures at the top and bottom were indicated based on the SsHsp20.1 and StHsp14.0 crystal structures. Abbreviations for sHSPs: SsHsp20.1 (*Sulfolobus solfataricus* Hsp20.1); TaHsp16.9 (*Triticum aestivum* Hsp16.9); MjHsp16.5 (*Methanocaldococcus jannaschii* Hsp16.5); SsHsp14.1 (*Sulfolobus solfataricus* Hsp14.1); StHsp14.0 (*Sulfolobus tokodaii* Hsp14.0). (For interpretation of the references to color in this figure legend, the reader is referred to the web version of this article.)

20 mM Tris–HCl, 150 mM NaCl pH 8.0) and reservoir solution (2% v/v tacsimate pH 7.0, 0.1 M HEPES pH 7.5, 16% w/v polyethylene glycol 3350). Crystals were mounted in loops and flash frozen in a nitrogen stream at 100 K in mother liquor containing 25% glycerol as cryoprotectant. Diffraction data were collected at the Shanghai SSRF BL17U1 beamline at 100K. The data were processed with HKL3000.

2.2. Structure determination

Hsp20.1 ACD structure was solved by molecular replacement using Phaser and the crystallographic structure of StHsp14.0 (PDB code 3AAB) as a search model. CNS/simulated-annealing was first performed for numbers of runs to improve the model quality. Then Phenix was used to refine the model and to obtain less biased 2Fo-Fc and Fo-Fc maps for model manual inspection and adjustment. Repeated rounds of manual refitting and crystallographic refinement were performed using COOT. Statistics of diffraction data processing and structure refinement are summarized in Supplementary Table 1.

2.3. Size exclusion chromatography assay

Oligomeric states of both wild-type proteins and variant proteins of Hsp20.1 and Hsp14.1 were examined with size-exclusion chromatography (SEC). SEC was performed using a Superdex 200 10/300 GL column (GE Healthcare Life Sciences) at a flow rate of 0.5 ml/min with absorbance monitored at 280 nm. The column was first equilibrated with the assay buffer (20 mM Tris–HCl, 150 mM NaCl pH 8.0), and then 200 μl of samples (1.0 mg/ml) were applied to the column. Standard proteins (ferritin, BSA and β-lactoglobulin) were used as molecular mass marker for calibration.

2.4. Analysis of chaperone activity

Chaperone activities of both wild-type proteins and variant proteins of Hsp20.1 and Hsp14.1 to inhibit MDH thermal aggregation were monitored by measuring the light scattering at 360 nm with a spectrophotometry. For each measurement, native MDH was incubated at 50 °C in the assay buffer (20 mM Tris–HCl, 150 mM NaCl pH 8.0) buffer in the presence or absence of sHsp (wild-type proteins or variant proteins). The molar ratio of sHsp (wild-type proteins or variant proteins) and MDH was 24:1.

3. Results

3.1. Structure of ACD of Sulfolobus solfataricus Hsp20.1

The Hsp20.1 structure was solved by the molecular replacement method, and refined at a resolution of 2.68 Å (Supplementary Table 1). There are two Hsp20.1 monomers in the asymmetric unit cells to form a dimer in crystal (Fig. 1A). Two monomers in a dimer have equivalent conformation; they can be well-superimposed on each other with the root mean-square deviations (RMSD) of 1.2 Å for the ACDs (residues 78–163). Each ACD of monomer possesses a typical β sandwich-fold configuration that consists of two antiparallel β-sheets, one β-sheet contains β-strands 2, 3, 9, and 8, the other β-sheet is form by β-strands 7, 5 and 4. However, the β6 strand is not observed in Hsp20.1 ACD structure (Fig. 1B). Almost all nonmetazoan sHSPs possess the β6 strand that locates in an extended loop and forms part of the dimeric interface (Fig. 1C). The β6 strand in the one subunit can interact with the β2-strand in the partner subunit through hydrogen bonds to stabilize nonmetazoan sHSP dimer. In the amino acid sequence of Hsp20.1, there are only four residues between strands β5 and β7. These residues form a much shorter loop that result in the loss of the distinct β6 strand.

3.2. Dimer interface of Hsp20.1

The β6 strand is also absent in all solved crystal structures of metazoan sHSPs, instead, a fused "β6+7" strand forms the dimer interface by interacting with the equivalent strand in the other subunit (Fig. 2A). However, dimer-forming interaction is not seen between "β6+7" strands of sHsp20.1 dimer. Hsp20.1 dimerization depends on ionic interactions as well as interbackbone hydrogen bonds that involve multiple charged or polar residues of ACD (Fig. 2B). Salt bridges between E101 in one subunit and R83 and R130 in the other subunit play a key role in monomer–monomer interaction to form the dimer. E101, R83 and R130 are not conservative

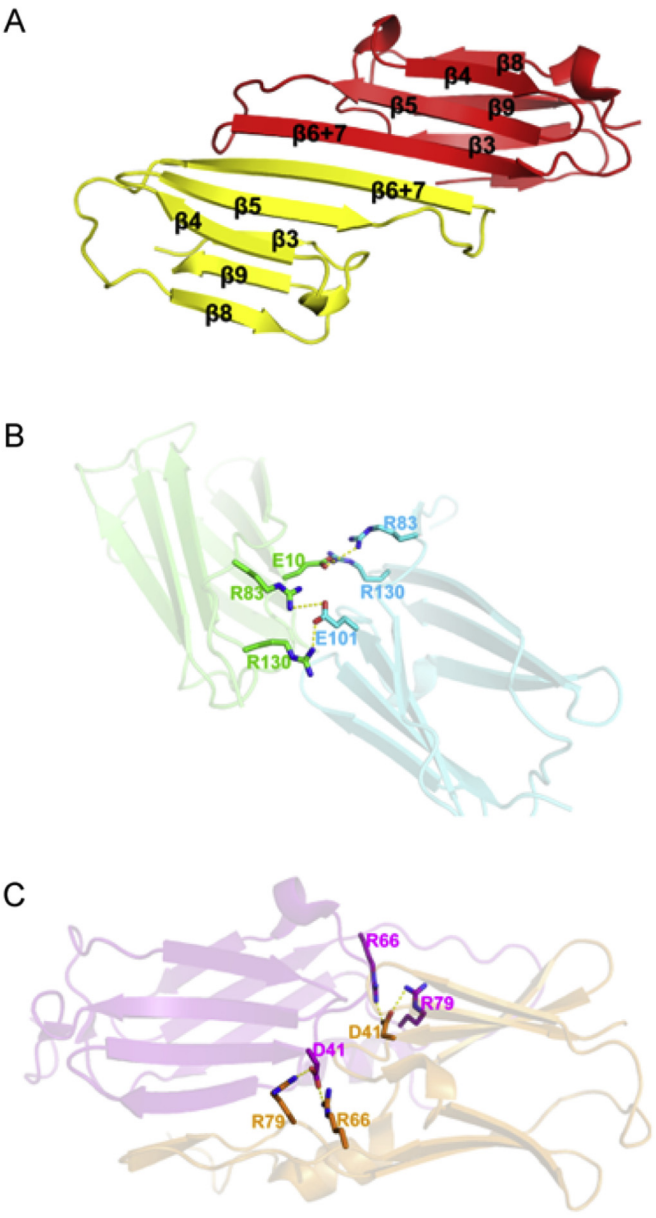

Fig. 2. Dimer interfaces of sHSPs. (A) The dimer of human αB-crystallin is formed by the interactions of β6+7 strands between two monomers (Protein Data Bank code 2WJ7). (B) Salt bridges are shown in the dimer interface of Hsp20.1. (C) Salt bridges are shown in the dimer interface of Hsp14.0.

amino acids in nonmetazoan sHSP sequences (Fig. 1C). In some nonmetazoan sHSPs, there are other charged residues that involve in forming salt bridges. As shown in Fig. 2C, D41, R66 and R79 participate in subunit contact in *Sulfolobus tokodaii* Hsp14.0 structure.

3.3. Characterization of IXI truncation mutant

To investigate the effect of the IXI motif on oligomer formation and chaperone activity, we prepared a mutant of Hsp20.1 ΔC8 (the last 8 residues including the IXI motif in the C-terminal extension were deleted). At first, the oligomeric states of Hsp20.1 wild-type (WT) and ΔC8 were examined by size exclusion chromatography (SEC). Hsp20.1 WT eluted in a symmetric peak about 480 kDa, consistent with an oligomer of 24 subunits. Whereas Hsp20.1 ΔC8 shown a peak of 40 kDa, corresponding to a dimer (Fig. 3A). Then, chaperone activity was examined by Light-scattering measurement. Hsp20.1 WT was able to protect porcine mitochondrial malate dehydrogenase (MDH) from thermal aggregation at 50 °C. Interestingly, Hsp20.1 ΔC8 could also inhibit the aggregation of MDH with efficiency comparable with that of the Hsp20.1 WT (Fig. 3C). These results indicate that the Hsp20.1 IXI motif is important for oligomerization but not for chaperone activity.

In contrast, we detected the influence of the IXI motif on quaternary structure and chaperone activity of the other *Sulfolobus solfataricus* small heat shock protein (Hsp14.1). Hsp14.1 wild-type (WT) formed a 24-mer that exhibited good chaperone activity at 50 °C, while Hsp14.1 ΔC8 (the last 8 residues including the IXI motif in the C-terminal extension were deleted) existed as small sub-oligomeric species that had lost the ability to suppress MDH thermal aggregation (Fig. 3B and D). These observations suggested that the IXI motif is essential for oligomerization and chaperone activity of Hsp14.1.

3.4. The N-terminal region is involved in binding clients

To determine whether the N-terminal region could affect the chaperone activity of Hsp20.1 WT and ΔC8, firstly, we constructed N-terminal truncation mutants of Hsp20.1 WT and ΔC8 (Hsp20.1 ΔN43 and ΔN43ΔC8), then we examined the thermal protection abilities of Hsp20.1 ΔN43 and ΔN43ΔC8 to MDH. As shown in Fig. 4, both Hsp20.1 ΔN43 and ΔN43ΔC8 could not prevent MDH thermal aggregation at 50 °C, considering that the N-terminal region is needed for Hsp20.1 WT and ΔC8 to bind substrates.

4. Discussion

Nonmetazoan sHSPs and metazoan sHSPs exhibit two very different dimer interfaces dependent on the presence or absence of β6 strand. In all determined nonmetazoan sHSP structures, such as *Methanocaldococcus jannaschii* Hsp16.5 and *Sulfolobus tokodaii* Hsp14.0, the β6 strand from one subunit forms dimeric interface through strand swapping with the β2 strand of the other subunit [7,9]. It has been shown that the β6 strand is required for dimerization. However, in our structure of the *Sulfolobus solfataricus* Hsp20.1 ACD, although the β6 strand is absent, the Hsp20.1 ACD also exists as a stable dimer. The Hsp20.1 ACD dimeric interface is formed by multiple charged or polar residues of ACD. Although several key residues in this interface are not fully conserved in nonmetazoan sHSP sequences, there are other charged or polar residues at their position that involve in subunit contacts in other

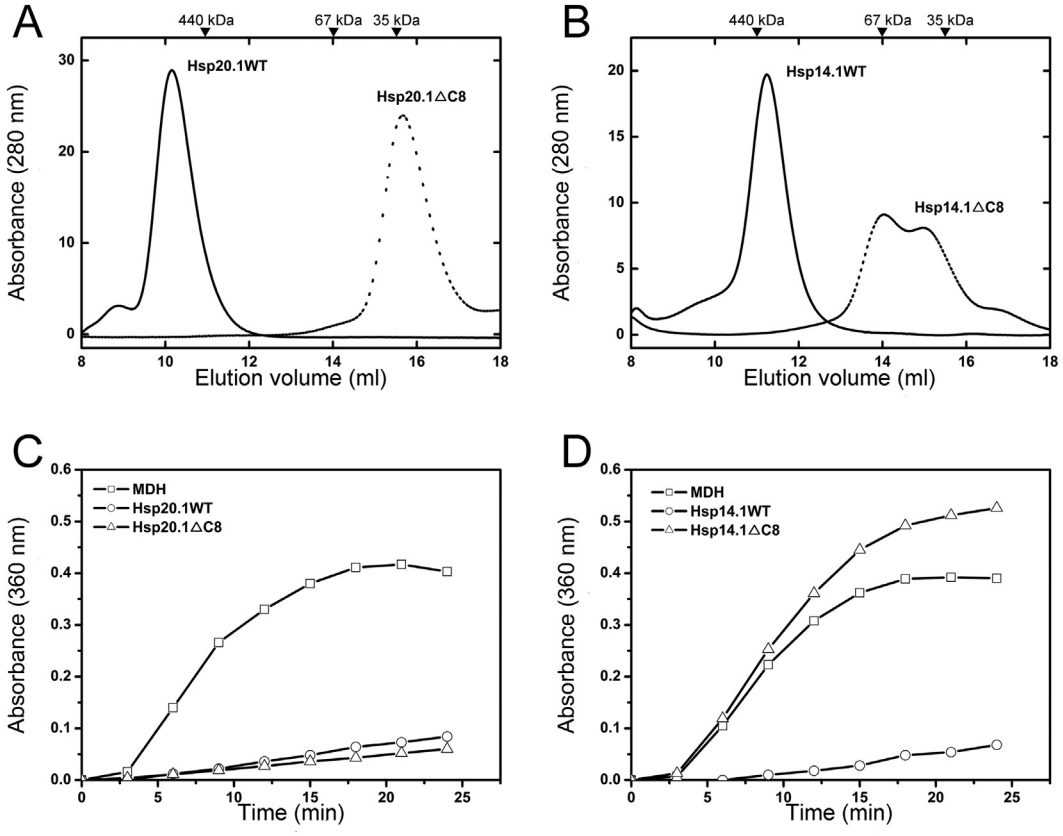

Fig. 3. The effect of IXI motif on the oligomeric states and chaperone activities of Hsp20.1 and Hsp14.1. (A) Size exclusion chromatographs of the Hsp20.1 wild type and Hsp20.1 ΔC8. Elution peak positions of the marker proteins were labeled above the profiles: ferritin (440 kDa), BSA (67 kDa) and β-lactoglobulin (35 kDa). (B) Size exclusion chromatographs of the Hsp14.1 wild type and Hsp14.1 ΔC8. (C) Chaperone activities of the Hsp20.1 wild type and Hsp20.1 ΔC8. (D) Chaperone activities of the Hsp14.1 wild type and Hsp14.1 ΔC8.

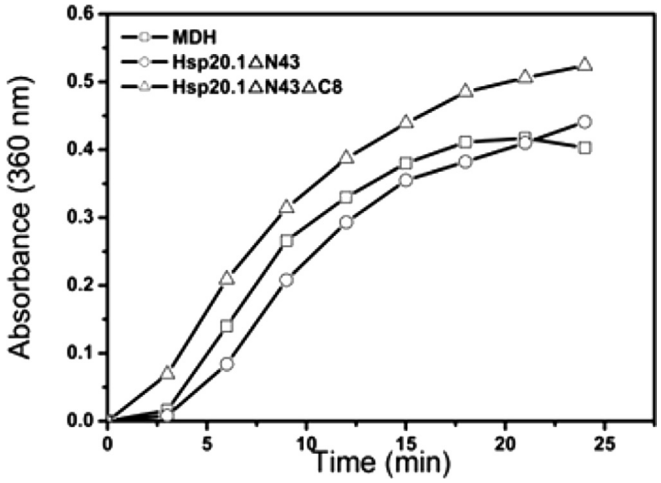

Fig. 4. The effect of N-terminal arm on the chaperone activities of Hsp20.1 oligomer and dimer. MDH was incubated at 50 °C in the presence or absence of Hsp20.1 ΔN43 or Hsp20.1 ΔN43ΔC8. The molar ratio of sHsp (Hsp20.1 ΔN43 or Hsp20.1 ΔN43ΔC8) and MDH was 24:1.

nonmetazoan sHSPs (Fig. 1C) [9,10]. Obviously, these observations may suggested that the β6 strand is not essential for forming dimeric interfaces in all nonmetazoan sHSPs. The presence of the β6 strand only contributes to additional stabilization of sHSP dimers.

The structures and chaperone activities of sHSP are usually strongly effected by environmental conditions. Therefore, the Hsp20.1 structure lacking the β6 strand may possess more structural variability. It has been shown that dimers are assembled by "β6+7" stands in metazoan sHSPs because of the absence of the β6 strand. Three different antiparallel (AP1, AP2 and AP3) dimer interfaces have been observed in vertebrate sHSP structures [20]. AP1, AP2 and AP3 dimer interfaces are likely sensitive to pH. Recent structure data revealed that pH may regulate a shift from AP2 to AP1 in αB-crystallin [18]. Therefore, it is believed that there are variations in the AP interface. The dynamic AP interface may contribute to the polydispersity and chaperone activity of αB-crystallin. Similarly, the Hsp20.1 dimer interface appears to have significant flexibility. On the one hand, Hsp20.1 comes from *sulfolobus solfataricus P2* that grows in the optimal pH (2–4) and optimum temperature (80 °C) [21]. Ionic interactions and hydrogen bonds in the Hsp20.1 dimer interface can be influenced by the low pH and the high temperature. Flexible structure is certainly needed for Hsp20.1 to tolerate extreme environment. On the other hand, dynamic exchange of subunits between oligomers allow suboligomers to bind to client. It is reported that dimer and monomer are important for initial complex formation in pea Hsp18.1 [22]. In the absence of β6 strand, Hsp20.1 is able to exchange subunits more rapidly, forming dimers or monomers capable of immediately recognizing and binding the unfolding proteins.

We have observed that the deletion of the IXI motif resulted in the disassembly of Hsp20.1 oligomers. Similar results were reported for almost all sHSPs, such as *Sulfolobus solfataricus* Hsp14.1 and *Sulfolobus tokodaii* Hsp14.0, except *Taenia saginata* Tsp36, which lacks the IXI motif (Fig. 3B) [23,24]. These findings indicate that interaction of the IXI motif with the β4-β8 groove is essential for connecting dimers to assemble higher order oligomer. Interestingly, the C-terminal truncation variant of Hsp20.1 (Hsp20.1 ΔC8) existed as a dimer but could also exhibit good chaperone activity suppressing MDH thermal aggregation at 50 °C. This observation coincides with the results of *Mycobacterium tuberculosis* Hsp16.3 and *Methanocaldococcus jannaschii* Hsp16.5 [14,25]. However, it is inconsistent with the findings of *Sulfolobus solfataricus* Hsp14.1 and *Sulfolobus tokodaii* Hsp14.0, in which the chaperone activity was significantly decreased once the oligomer was disrupted by deleting the IXI motif (Fig. 3D) [23]. It is possible that there are two substrate binding models that exist in different sHSPs under the thermal stress. One model depends on the oligomeric architecture to hold substrate, while the other just needs only a dimer to bind the substrate.

Our data also indicate that the N-terminal region is involved in binding of the substrate. The removal of the 43 N-terminal residues significantly affected the chaperone activities of Hsp20.1 WT and Hsp20.1 ΔC8. Both Hsp20.1 ΔN43 and Hsp20.1 ΔN43ΔC8 failed to protect MDH from thermal aggregation at 50 °C, revealing that both oligomer (Hsp20.1 WT) and dimer (Hsp20.1 ΔC8) used the N-terminal regions to interact with unfolded substrates. Understanding in detail how these interactions are accomplished is crucial to explaining clearly the thermal protection mechanism of sHSP [11,26]. Unfortunately, we were not able to obtain the Hsp20.1 structure that contained the full N-terminal region, although we attempted to crystalize a lot of constructs. The inability to obtain structural information is certainly resulted by the flexibility of the N-terminal arm [27]. Of the available X-ray structures, full or half of N-terminal arms are also not resolved [1]. However, the N-terminal arm appear to exist as helix that is suggested by the partial N-terminal region structure of *Triticum aestivum* Hsp16.9 as well as the cryo-electron microscopy study on *Methanocaldococcus jannaschii* Hsp16.5 [10,28]. Recent report indicates that the N-terminal region is likely to undergo a disorder-to-helix transition that is regulated by environment conditions [9]. The amphiphilic helices have advantages for adapting substrates of various sizes and shapes. Therefore, further studies should put more emphasis on the N-terminal conformation transitions.

Conflict of interest

There is no conflict of interest.

Acknowledgments

This project was supported by the Fundamental Research Funds for the Central Universities (2014ZM0062) and PhD Start-up Fund of Natural Science Foundation of Guangdong Province (No. S2012040007734).

Appendix A. Supplementary data

Supplementary data related to this article can be found at http://dx.doi.org/10.1016/j.bbrc.2015.01.134.

Transparency document

Transparency document related to this article can be found online at http://dx.doi.org/10.1016/j.bbrc.2015.01.134.

References

[1] E. Basha, H. O'Neill, E. Vierling, Small heat shock proteins and alpha-crystallins: dynamic proteins with flexible functions, Trends Biochem. Sci. 37 (2012) 106–117.
[2] T.L. Tapley, T.M. Franzmann, S. Chakraborty, U. Jakob, J.C. Bardwell, Protein refolding by pH-triggered chaperone binding and release, Proc. Natl. Acad. Sci. U. S. A. 107 (2010) 1071–1076.
[3] N.S. Rajasekaran, P. Connell, E.S. Christians, L.J. Yan, R.P. Taylor, A. Orosz, X.Q. Zhang, T.J. Stevenson, R.M. Peshock, J.A. Leopold, W.H. Barry, J. Loscalzo, S.J. Odelberg, I.J. Benjamin, Human alpha B-crystallin mutation causes oxido-reductive stress and protein aggregation cardiomyopathy in mice, Cell 130 (2007) 427–439.

[4] M. Haslbeck, T. Franzmann, D. Weinfurtner, J. Buchner, Some like it hot: the structure and function of small heat-shock proteins, Nat. Struct. Mol. Biol. 12 (2005) 842–846.
[5] G.R. Hilton, H. Lioe, F. Stengel, A.J. Baldwin, J.L. Benesch, Small heat-shock proteins: paramedics of the cell, Top. Curr. Chem. 328 (2013) 69–98.
[6] N. Kourtis, V. Nikoletopoulou, N. Tavernarakis, Small heat-shock proteins protect from heat-stroke-associated neurodegeneration, Nature 490 (2012) 213–218.
[7] K.K. Kim, R. Kim, S.H. Kim, Crystal structure of a small heat-shock protein, Nature 394 (1998) 595–599.
[8] S.P. Delbecq, S. Jehle, R. Klevit, Binding determinants of the small heat shock protein, alphaB-crystallin: recognition of the 'IxI' motitf, EMBO J. 31 (2012) 4587–4594.
[9] K. Takeda, T. Hayashi, T. Abe, Y. Hirano, Y. Hanazono, M. Yohda, K. Miki, Dimer structure and conformational variability in the N-terminal region of an archaeal small heat shock protein, StHsp14.0, J. Struct. Biol. 174 (2011) 92–99.
[10] R.L. van Montfort, E. Basha, K.L. Friedrich, C. Slingsby, E. Vierling, Crystal structure and assembly of a eukaryotic small heat shock protein, Nat. Struct. Biol. 8 (2001) 1025–1030.
[11] N. Jaya, V. Garcia, E. Vierling, Substrate binding site flexibility of the small heat shock protein molecular chaperones, Proc. Natl. Acad. Sci. U. S. A. 106 (2009) 15604–15609.
[12] A. Soto, I. Allona, C. Collada, M.A. Guevara, R. Casado, E. Rodriguez-Cerezo, C. Aragoncillo, L. Gomez, Heterologous expression of a plant small heat-shock protein enhances Escherichia coli viability under heat and cold stress, Plant Physiol. 120 (1999) 521–528.
[13] K. Usui, O.F. Hatipoglu, N. Ishii, M. Yohda, Role of the N-terminal region of the crenarchaeal sHsp, StHsp14.0, in thermal-induced disassembly of the complex and molecular chaperone activity, Biochem. Biophys. Res. Commun. 315 (2004) 113–118.
[14] R. Kim, L. Lai, H.H. Lee, G.W. Cheong, K.K. Kim, Z. Wu, H. Yokota, S. Marqusee, S.H. Kim, On the mechanism of chaperone activity of the small heat-shock protein of Methanococcus jannaschii, Proc. Natl. Acad. Sci. U. S. A. 100 (2003) 8151–8155.
[15] Y. Hanazono, K. Takeda, M. Yohda, K. Miki, Structural studies on the oligomeric transition of a small heat shock protein, StHsp14.0, J. Mol. Biol. 422 (2012) 100–108.
[16] S. Jehle, P. Rajagopal, B. Bardiaux, S. Markovic, R. Kuhne, J.R. Stout, V.A. Higman, R.E. Klevit, B.J. van Rossum, H. Oschkinat, Solid-state NMR and SAXS studies provide a structural basis for the activation of alphaB-crystallin oligomers, Nat. Struct. Mol. Biol. 17 (2010) 1037–1042.
[17] E. Hilario, F.J. Martin, M.C. Bertolini, L. Fan, Crystal structures of Xanthomonas small heat shock protein provide a structural basis for an active molecular chaperone oligomer, J. Mol. Biol. 408 (2011) 74–86.
[18] A.R. Clark, C.E. Naylor, C. Bagneris, N.H. Keep, C. Slingsby, Crystal structure of R120G disease mutant of human alphaB-crystallin domain dimer shows closure of a groove, J. Mol. Biol. 408 (2011) 118–134.
[19] G.K. Hochberg, H. Ecroyd, C. Liu, D. Cox, D. Cascio, M.R. Sawaya, M.P. Collier, J. Stroud, J.A. Carver, A.J. Baldwin, C.V. Robinson, D.S. Eisenberg, J.L. Benesch, A. Laganowsky, The structured core domain of alphaB-crystallin can prevent amyloid fibrillation and associated toxicity, Proc. Natl. Acad. Sci. U. S. A. 111 (2014) E1562–E1570.
[20] E.V. Baranova, S.D. Weeks, S. Beelen, O.V. Bukach, N.B. Gusev, S.V. Strelkov, Three-dimensional structure of alpha-crystallin domain dimers of human small heat shock proteins HSPB1 and HSPB6, J. Mol. Biol. 411 (2011) 110–122.
[21] Q. She, R.K. Singh, F. Confalonieri, Y. Zivanovic, G. Allard, M.J. Awayez, C.C. Chan-Weiher, I.G. Clausen, B.A. Curtis, A. De Moors, G. Erauso, C. Fletcher, P.M. Gordon, I. Heikamp-de Jong, A.C. Jeffries, C.J. Kozera, N. Medina, X. Peng, H.P. Thi-Ngoc, P. Redder, M.E. Schenk, C. Theriault, N. Tolstrup, R.L. Charlebois, W.F. Doolittle, M. Duguet, T. Gaasterland, R.A. Garrett, M.A. Ragan, C.W. Sensen, J. Van der Oost, The complete genome of the crenarchaeon Sulfolobus solfataricus P2, Proc. Natl. Acad. Sci. U. S. A. 98 (2001) 7835–7840.
[22] F. Stengel, A.J. Baldwin, A.J. Painter, N. Jaya, E. Basha, L.E. Kay, E. Vierling, C.V. Robinson, J.L. Benesch, Quaternary dynamics and plasticity underlie small heat shock protein chaperone function, Proc. Natl. Acad. Sci. U. S. A. 107 (2010) 2007–2012.
[23] H. Saji, R. Iizuka, T. Yoshida, T. Abe, S. Kidokoro, N. Ishii, M. Yohda, Role of the IXI/V motif in oligomer assembly and function of StHsp14.0, a small heat shock protein from the acidothermophilic archaeon, Sulfolobus tokodaii strain 7, Proteins 71 (2008) 771–782.
[24] R. Stamler, G. Kappe, W. Boelens, C. Slingsby, Wrapping the alpha-crystallin domain fold in a chaperone assembly, J. Mol. Biol. 353 (2005) 68–79.
[25] X. Fu, H. Zhang, X. Zhang, Y. Cao, W. Jiao, C. Liu, Y. Song, A. Abulimiti, Z. Chang, A dual role for the N-terminal region of Mycobacterium tuberculosis Hsp16.3 in self-oligomerization and binding denaturing substrate proteins,, J. Biol. Chem. 280 (2005) 6337–6348.
[26] J. Shi, H.A. Koteiche, E.T. McDonald, T.L. Fox, P.L. Stewart, H.S. McHaourab, Cryoelectron microscopy analysis of small heat shock protein 16.5 (Hsp16.5) complexes with T4 lysozyme reveals the structural basis of multimode binding, J. Biol. Chem. 288 (2013) 4819–4830.
[27] S. Jehle, B.S. Vollmar, B. Bardiaux, K.K. Dove, P. Rajagopal, T. Gonen, H. Oschkinat, R.E. Klevit, N-terminal domain of alphaB-crystallin provides a conformational switch for multimerization and structural heterogeneity, Proc. Natl. Acad. Sci. U. S. A. 108 (2011) 6409–6414.
[28] H.A. Koteiche, S. Chiu, R.L. Majdoch, P.L. Stewart, H.S. McHaourab, Atomic models by cryo-EM and site-directed spin labeling: application to the N-terminal region of Hsp16.5, Structure 13 (2005) 1165–1171.